Assessment of Morphological Dynamics in Ibajay, Aklan Coast using Delft3D Numerical Simulation

Dominic M. Bautista*, Eric C. Cruz, and Eugene C. Herrera
Institute of Civil Engineering, College of Engineering,
University of the Philippines, Diliman, Quezon City, 1101, Philippines
*Corresponding Author: dmbautista2@up.edu.ph

Abstract – The Philippines has dynamically active coastal areas where sediment transport is a matter of concern due to its environmental implications, one of which is coastal erosion. Local studies have used seasonal beach profiling, shoreline tracing, and bathymetric analysis to provide relevant information on possible causes, trends, and adaptation strategies to address coastal erosion, but studies using numerical modelling of morphological dynamics are limited despite its capability to quantify different processes that is essential when an engineering intervention is necessary. This study uses numerical modelling in assessing coastal erosion and aims to model the hydrodynamics, waves, sediment transport and morphological dynamics of the study area using Delft3D. A 3-dimensional, coupled FLOW and WAVE model was set-up and calibrated to assess the transport of sediments and morphological dynamics in Ibajay, Aklan, one of the areas tagged as experiencing coastal erosion due to the presence of identifying physical features. The model was calibrated by comparing simulation results with measured time-series water level, bottom velocity, and wave parameters obtained from field surveys. Good agreement with measured parameters was observed after calibration, with root-mean-square-error of less than 10% of range of observed values at an observation point located 100 m off the coast at a depth of 8 m. The calibrated model was run for one year under prevailing (non-extreme) wind and wave conditions. Results showed two transport patterns caused by breaking of waves and strong currents near the lateral boundaries. It was determined that the shore is accreting with some erosion observed on the lateral boundaries caused by tidal asymmetry. Dry season months from November to April exhibited more active cross-shore transport due to intensifying of waves brought by the northeast monsoon while recovery of sand was observed during calmer conditions the rest of the year.

Keywords: coastal erosion, morphological dynamics, sediment transport, numerical simulation, Delft3D

I. INTRODUCTION

The Philippines has vast amount of natural water resources. With more than 36,000 kilometers of coastline, 50% of the country's municipalities are within the 1-kilometer boundary from the coast where 62% of the population lives [1]. These numbers signify the importance of coastal resources and the necessity to properly manage it. While the country has significant benefits from its natural geographic setting, it is also exposed to different kinds of natural hazards such as typhoons, earthquakes, coastal erosion, among others. These hazards contribute to 88.4% of the average annual damages of 38.58 billion pesos caused by disasters which is why proper planning and execution of risk management strategies are necessary in order to minimize the losses [2]. Coastal erosion, or the loss of land causing the shoreline to

retreat inland, is a complex problem driven by natural (e.g. wind and waves, longshore currents) and anthropogenic (e.g. groundwater extraction, wetland conversion, dredging) factors [3]. With the archipelagic nature of the country, many areas are susceptible to coastal erosion due to vast tidal and wave exposure and intense storms that move coastal sediments on a regular basis. In fact, at least 20 areas around the Philippines are reportedly experiencing or experienced coastal erosion based on physical observations along the coast [4]. Some areas with documented observations of coastal erosion are in La Union [5], Bataan [6], Leyte [7], and Iloilo [8].

The study of the movement of sediments in the coastal environment has been the subject of several studies due to its environmental implications. Sediments transporting away from a certain area may cause erosional damage due to loss of land. On the other hand, sediment deposition may be damaging to channels and harbors and may affect the existing ecosystem in the body of water. In addition, sediments also act as "contaminant traps" that can store pollutants for significant amount of time. With these effects in the natural environment, it is therefore imperative to understand the dispersal patterns of coastal sediments in terms of local and regional coastal planning and management for resource development [9]. In Manila Bay, Siringan and Ringor [10] analyzed the bay's sediment dynamics by studying bathymetry changes from 1944 to 1961. In La Union, Berdin, et al. [11] used time-series analysis of maps and images, coupled with social surveys to analyze changes in shoreline positions over decadal time scales. They overlayed digitized shoreline positions from old maps and from a Global Positioning System (GPS) survey with average accuracy of ±8 meters. In Cavite, Doruelo [12] conducted a multi-method investigation of the coastal sediment dynamics. For offshore sediment transport patterns, granulometric analysis was conducted while nearshore sedimentation was modeled by integrating wave refraction data with records of bathymetric and shoreline changes. In Leyte, Soria et al. [13] described the spatial variation of sediments caused by Typhoon Haiyan by analyzing the sediment overwash deposits inland. Also in the same event, Doctor [14] investigated the shoreline response of the Eastern Leyte coast and identified long-term forcing mechanisms that promoted the recovery of sand. Other coastal erosion studies in the Philippines were done in Guimaras, Bantayan Island in Cebu, Malay in Aklan, Bolinao in Pangasinan, Davao, and some coastlines in Bicol region [3].

In existing studies, coastal erosion was identified and analyzed based on five different methodologies. Usage of photo or video documentation of seasonal coastal changes can provide significant shoreline qualities or features that can indicate coastal erosion. Beach profiling is another method used wherein measurements of the cross-shore profile (perpendicular to the shoreline orientation) of a beach were taken. In this method, the distance and difference in elevation between two graduated rods of the same height were measured starting from an inland reference point moving out towards the sea. By taking the beach profile, a visual representation in terms of the changing shape of the beach, as well as measurable changes in the volume of sediments lost or gained can be produced and analyzed. Another method, called shoreline tracing, is the process of walking along the coast (waterline) with a handheld GPS to trace the location of the shoreline. This simple mapping method, however, must be corrected for daily tidal fluctuations as the shoreline varies between the low tide line and high tide line. Both beach profiling and shoreline tracing method are usually done hand in hand every season to monitor changes in the longshore and cross-shore properties of the study

coastline. Another method used in assessing coastal erosion is by overlaying multiple topographic (and bathymetric) maps from different time scales (usually decadal) and comparing the position of the shoreline. These maps can be obtained from national agencies such as the National Mapping and Resource Information Authority (NAMRIA), from global datasets such as the General Bathymetric Chart of the Oceans (GEBCO), or from actual bathymetric surveys. Finally, anecdotal accounts can be used as valuable sources of information that can fill the gap provided by limited coverage of maps and images. It involves interviewing long-time coastal residents with good recall of coastal changes in their locality. All the methods mentioned proved to be sufficient in providing possible causes, trends, and adaptation strategies about coastal erosion. However, these methods lack the capacity to integrate appropriate engineering solutions that can address coastal erosion in the long term. Typical interventions employed are constructing hard structures such as groins and revetments [15] and nature-based solutions such as mangrove forests and seagrass meadows [16], both of which require detailed analysis of the existing coastal processes in order to arrive at an appropriate design and effectiveness of the solution. This is where numerical modelling can be utilized. Numerical simulation of coastal processes can provide detailed characterization of the hydrodynamics, waves, and sediment transport, along with generation of various scenarios that can predict the implications of the proposed solution to the coastal environment, and later on to the overall sustainable management strategy against coastal erosion [17].

The main objective of the study is to assess the coastal sediment dynamics and morphological changes through the simulative analysis of the hydrodynamics, waves, and sediment transport of the study area under prevailing conditions using the Delft3D modelling platform. A calibrated hydrodynamic-wave model coupled with sediment transport model was created to characterize these processes in the coastal zone. The dominant tidal hydrodynamics and prevailing wave climate were described and areas of erosion and accretion were identified based on simulated sediment transport patterns and changes in morphology.

II. METHODOLOGY

2.1 Study Area

The study area of this research is one of the identified coastal erosion prone areas located on the northwestern coast of Panay Island, see Figure 1. The coastline is 4.7 km long and spans from 122º10'33.81" E longitude, 11º49'9.21" N latitude to 122º12'54.99" E longitude, 11º48'37.87" N latitude located within the barangays of Naisud and Bugtongbato in the municipality of Ibajay, Aklan. Ibajay is a 3rd class municipality where residents rely mostly on fishing as a source of livelihood. Houses made of light materials can be seen as close as 5 to 10 meters from the beach along with fishing boats that are parked on several segments along the coast. On the west, an incomplete concrete wharf bounds the coast while a headland can be seen on the east. A small stream passing through the natural mangrove forest of Katunggan It Ibajay (KII) Ecopark discharges into the Sibuyan Sea midway of the concave shoreline. The climate in the study area is classified as Type III where no period of maximum rains is pronounced and the dry season lasts for three months from March to May. During December to February, northeast monsoon winds from the side of Sibuyan Sea are prevalent generating intensified waves. The tidal pattern is mixed semidiurnal with range that reach up to 2.2 meters

during spring tide. Sediments along different segments of the coast are visually uniform and composed primarily of sand. Figures 1d and 1e show two areas along the coast where physical indicators of coastal erosion such as scarps and exposed roots of coconut trees have been observed. This signifies that the area could have been experiencing coastal erosion.
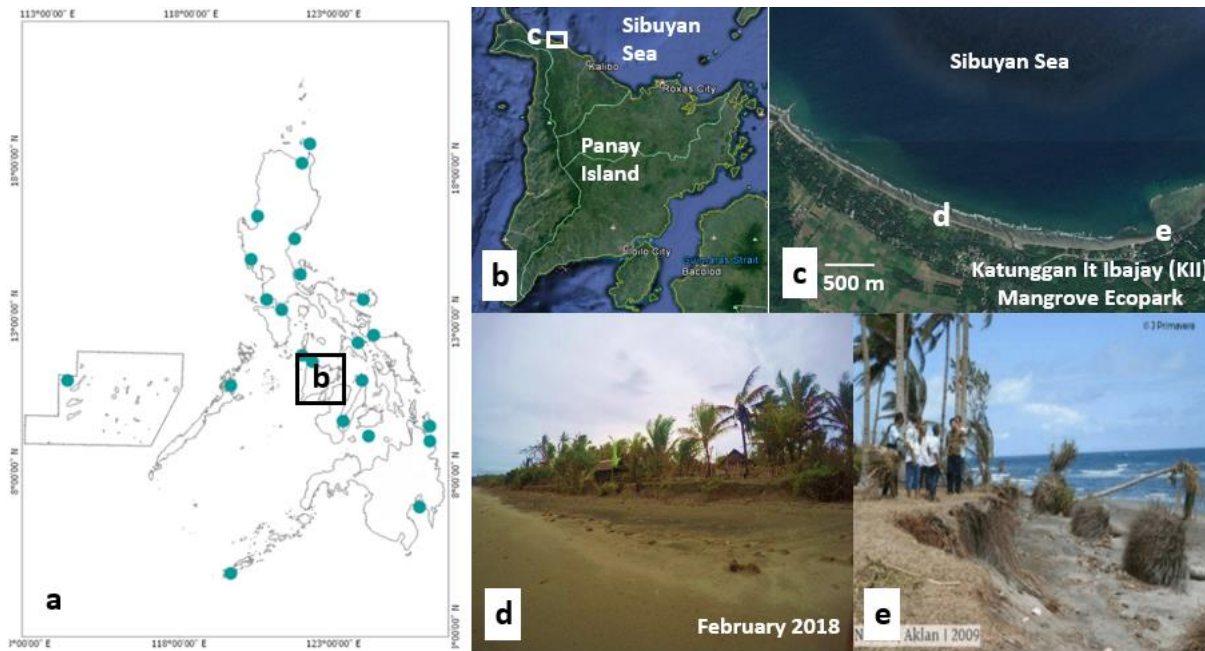
Figure 1. Research study area in Ibajay, Aklan: (a) Philippine map showing areas (green dots) where coastal erosion is observed [5], (b) Panay Island, (c) Ibajay coastline, (d) and (e) areas along the coastline where physical indicators of coastal erosion, such as scarps and exposed tree roots, were documented

2.2 Data Gathering

   Three fieldworks were conducted in September 2017, November 2017, and February 2018 with the objective of gathering primary data in the study site. Secondary data, on the other hand, were either requested from government agencies or downloaded from available global databases online. Table 1 summarizes the data collected in this study and how they were used in this research. In addition, information on relevant points where data were gathered are also described. The location of these points relative to the study area are shown in Figure 2.

Figure 2. Locations where data were gathered for the study

2.3 Numerical Model

The Delft3D modelling suite was used in this study. It is an integrated system consists of a number of modules which together, provides built-in coupling of hydrodynamics, waves, and sediment transport. The hydrodynamic model, Delft3D-FLOW, solves the 2- or 3-dimensional Navier-Stokes equations for an incompressible fluid under the shallow water, Boussinesq, and hydrostatic pressure assumptions. The system of equations consists of the horizontal momentum equations, the continuity equation, the transport equation, and a turbulence closure model are solved using an alternating direction implicit (ADI) method on a finite difference grid [18].

The wave model, Delft3D-WAVE, is based on the third-generation SWAN (Simulating Waves Nearshore) wave model of Booij et al. [19]. It is based on the discrete spectral action balance equation which simulates the evolution of wind-generated waves in coastal waters accounting for wind growth, wave refraction, wave-wave interactions, and dissipation. The discrete spectral action balance equation is solved in SWAN using an implicit upwind finite difference scheme in five dimensions (time, physical space, and spectral space) on a structured grid.

The sediment transport and morphology models are incorporated in the Delft3D-FLOW module. It supports both bedload and suspended load transport of non-cohesive and cohesive sediments but are treated separately in the numerical solution. In this study, only non-cohesive transport was activated as the sediments in the study area are primarily made up of sand. Non-cohesive transport in Delft3D uses the formulas developed by Van Rijn [20]. A reference height "a" is defined to separate bed load (below a) and suspended load (above a). Suspended

sediment transport is obtained by solving the advection-diffusion equation. Sediment settling velocity is accounted using a diameter-dependent method. On the other hand, bedload transport for simulations including waves is approximated using the Van Rijn [21] formulation.

Delft3D-FLOW and Delft3D-WAVE account for wave-current interaction processes by the means of online coupling. All three models can run simultaneously wherein the hydrodynamic model and the wave model will exchange calculated results with each other while sending these results to the sediment transport model. This process is particularly important for sediment dynamics to account for additional mass flux due to waves, turbulence increase due to breaking of waves, and enhancement of bed shear stress.

2.4 Model Set-up
  2.4.1   Computational Domains

Three computational grids were created in this study, each with varying resolution and were nested with each other as shown in Figure 3. The regional domain is the largest that is a purely hydrodynamic, structured grid that covers the northern Visayas region from the West Philippines Sea on the left boundary to the Pacific Ocean on the right. The local domain is a tilted rectangular grid that is parallel to the northern Panay coast extending up to the center of Sibuyan Sea. It is a coupled hydrodynamic-wave model. The nearshore domain is a curvilinear grid that follows the shape of the study coastline extending up to 2 kilometers off the study coast. It is also a coupled hydrodynamic-wave model with the sediment transport module of Delft3D-FLOW activated. One-way nesting was implemented wherein each model was ran separately using the output of the larger domain as boundary conditions to the smaller domain, that is, from regional to local and from local to nearshore. Both the regional and local domains are 2-dimensional as their sole purpose is to provide the necessary boundary conditions for the nearshore domain. On the other hand, the nearshore domain is 3-dimensional to better analyze the bottom velocities that cause the movement of sediments in the bed. The nearshore domain is divided into 3 layers with thickness of 25% at the surface, 50% at the middle, and 25% at the bottom. Table 2 summarizes the properties of the three computational domains.
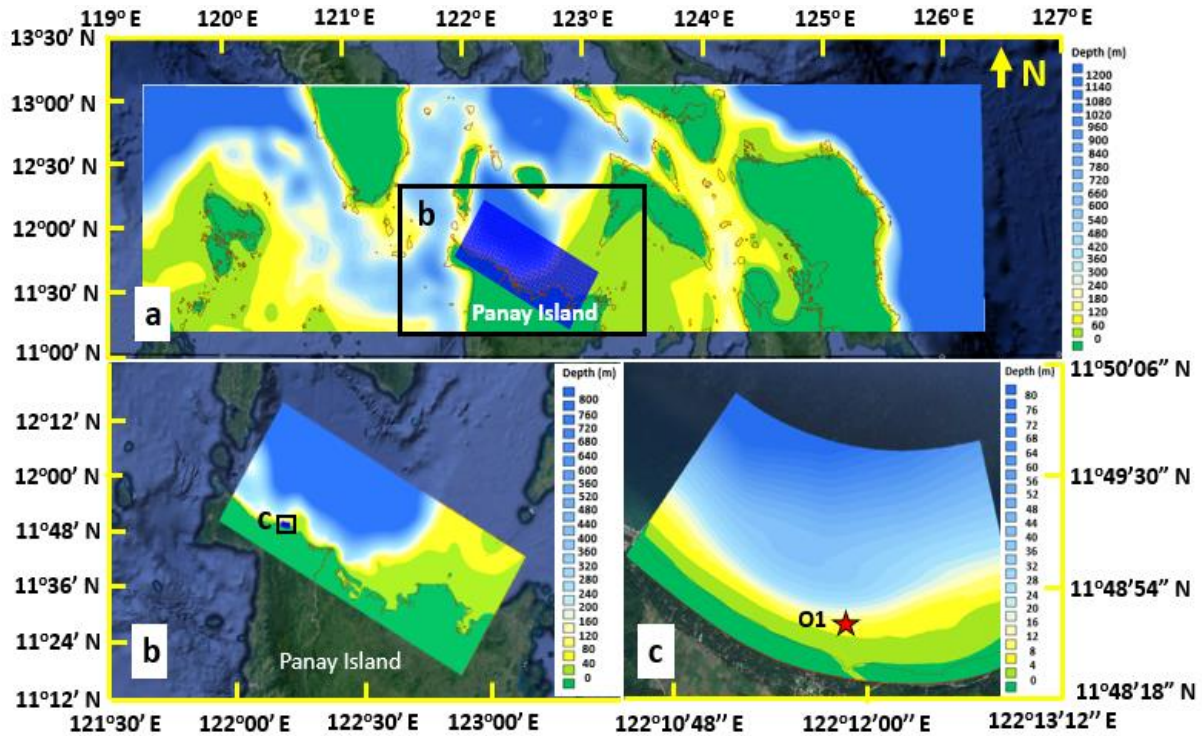
Figure 3. Computational domains used in the study: (a) regional, (b) local, (c) nearshore
(location of calibration point O1 is indicated)

2.4.2   Time Frame and Boundary Conditions

The simulation period lasted from August 1, 2017 00:00:00 UTC to August 1, 2018 00:00:00 UTC on all computational domains. A one-year simulation period is necessary to capture the monthly and seasonal variations of the coastal processes within the study area. The time step differed on each computational grid depending on the numerical stability requirement of Delft3D-FLOW. A time step of 1.5 s, 60 s, and 3 s, were used for the regional, local, and nearshore model, respectively. The coupling time between Delft3D-FLOW and Delft3D-WAVE is every 3 hours, which is the interval of wave boundary data used in the simulation.

The boundary conditions on each computational domain were assigned on all segments that have a depth of greater than zero. In the purely hydrodynamic regional model, several segments were selected as open boundaries where water level values, based on different astronomic tide constituents (amplitudes and phases), were applied. Longer open boundaries were discretized into smaller segments of 30 km to sufficiently capture the variation of water level. In the local domain, the discretization of the open boundaries were every 12 km and time-series water level values came from the results of the regional domain simulation through the built-in nesting program of Delft3D. Wave boundary on the local domain was set up as a constant, time-varying value on the segment located on Sibuyan Sea. The boundary conditions in the nearshore domain were time-series water level data and wave parameters from the simulation results of the local domain. Due to the additional sediment process, transport conditions at the open boundaries were also specified and were set to be the equilibrium concentration profile of sand. This means that the sediment load entering through the boundaries were adapted based on the local flow conditions determined by the model.

2.4.3 Physical Parameters

The physical parameters used in the model are summarized in Table 3. Physical parameters that are not included in the summary were set to default values specified by Delft3D. These parameters either do not have an effect on model results or their effects cannot be analyzed by sensitivity analysis due to lack of available data (e.g. wave breaking parameters).

Variation of bed roughness on the regional model affected the amplitude and phase of the modeled time-series water level on O1, CL, and LB. A depth-dependent value for the bed roughness was used to increase the effect of the parameter on deeper portions of the domain. The wind input for the local model was averaged from the data forecasted on SS and the measured data on KC since using SS data overestimated the wave heights observed on O1 while using KC data underestimated it. The whitecapping formulation of Komen et al. [22] was used as it depends on the spectrally averaged wave steepness that includes swell, a wave frequency that is included in the wave boundary used in the model. Directional spreading affects the distribution of wave height in the domain and a constant value of 10° was found to be optimal based on sensitivity analysis. The wind drag coefficient used was linearized from the results of the study of Zijlema et al. [23] as shown in Figure 4. The linearization was necessary to account for the limitation in numerical modelling of wind shear stress in Delft3D where the wind speed-dependence of the drag coefficient can only be defined using a piecewise function of two linear equations with 3 breakpoints. The bottom friction coefficient for wave dissipation was also adopted from Zijlema et al. [23]. The bed roughness on the nearshore model was adjusted as it affects the magnitude of the bottom velocity. A depth-dependent value was adopted assuming a typical depth of closure of 20 m where sediments beyond remained undisturbed. The horizontal eddy viscosity is a calibration parameter that affects the timing and direction of the velocity due to its effect in the turbulence closure model of Delft3D. A value of 5 m^2/s was adopted after a series of trial and error during sensitivity analysis. Sediment information coming from the stream discharge is assumed zero since the quality of sediments coming out from the watershed is organic silt and clay from the mangrove forest. These sediments were not observed along the coast and therefore neglected in the simulation.
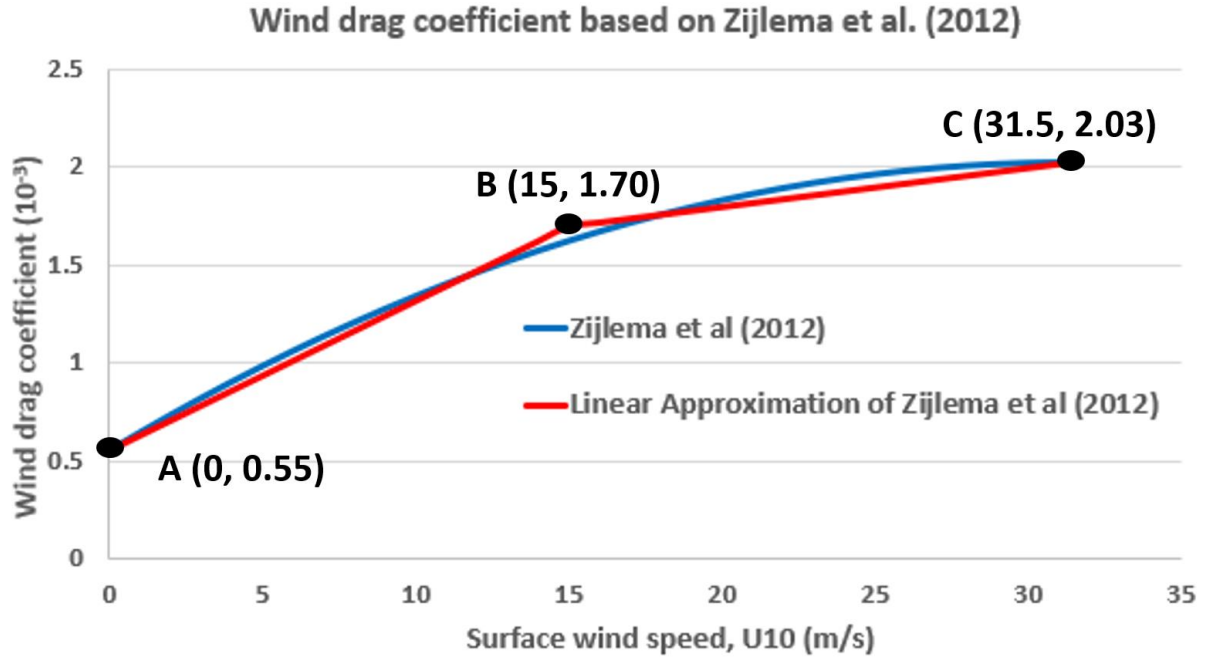
Figure 4. Wind drag coefficient used in the study indicating the 3 breakpoints A, B, and C ($U10$, C_D) entered to Delft3D

Sieve analysis of the sample taken from the study coast showed that the sand is uniformly graded with a median diameter of 0.223 mm. This implies that a single sediment fraction is sufficient to represent the sediments collected. A constant representation of all the sediments in the study area was assumed based on visual observation of the sandy coast during the field surveys. The option to update the bathymetry on each time step was activated to account for the changes in bathymetry over time. The rest of the parameters for the sediment transport and morphology module were set to default values.

2.5 Calibration and Validation

The level of agreement between observed and modelled time-series data were assessed by calculating the root-mean-square error (RMSE). RMSE is a statistical parameter that represents the accuracy between observed and simulated data. Lower values of RMSE indicate less residual variance and therefore, better model performance. The RMSE can be calculated using Equation (1).

$$RMSE = \sqrt{\frac{1}{N}\sum_{i=1}^{N}(S_i - O_i)^2} \tag{1}$$

where N is the total number of data points, S_i is the simulated data, and O_i is the observed data. The level of accuracy provided by the RMSE value was compared with the performance guidelines for hydrodynamic and wave models established by Williams and Esteves [24] shown in Table 4.

III. RESULTS AND DISCUSSION

3.1 *Calibration and Validation Results*

Results of the calibration and validation of the nearshore model are summarized in Table 5 while Figure 5 shows the comparison of different parameters analyzed. Figures 5a, 5c, and 5e are water level and bottom velocity results from calibration, while 5b, 5d, and 5f, are the results when the model was run on a different time period for validation. Figures 5g and 5h are wave height and wave period, respectively, obtained from the same validation period. Except for the validation of water level values, all parameters listed in Table 4 satisfied the prescribed performance guidelines in terms of RMSE. Despite the underestimation of the peak water level values during the validation period, the timing of the tide was captured as shown in Figure 5b and the obtained RMSE is still within the acceptable value of 10% of the spring tide range. Thus, it was concluded that the numerical model sufficiently captures the physical processes within the nearshore domain. Calibration of the sediment transport model was not performed due to lack of actual data that can be compared to numerical simulation results. Despite this, the use of calibrated forcings (waves and currents) is sufficient to predict erosion and deposition patterns in the study area [25].

3.2 *Dominant Tidal Hydrodynamics*

Tidal forcing dominates the water fluctuations in the study area. Spatially, water level values do not vary anymore due to the limited area of the nearshore domain. Similar to the simulated water levels, the variation of velocity within the nearshore model is greatly dominated by tidal forcing. As shown in Figure 6, two distinct patterns were observed based on model simulations which follow the timing of flood-ebb tide cycle. During ebb tide, fast-moving currents from the lateral boundaries, with magnitude of more than 0.8 m/s, meet towards the center of the domain and exits towards north. A small circulation, located at the northwestern side of the domain is created and moves towards the north boundary until it dissipates when the flow reverses during flood tide. On the other hand, flood tide currents enter from the north boundary and exit at the same lateral boundaries at relatively slower speeds than when it enters during ebb tide. This tidal flow asymmetry is a recurring pattern throughout the entire long-term simulation and is found to be dependent on the water level fluctuation according to the principle of continuity. The lower the water level during the ebb tide transition, the faster the currents become. On the other hand, the higher the water level is during the flood tide transition, the slower the currents are.
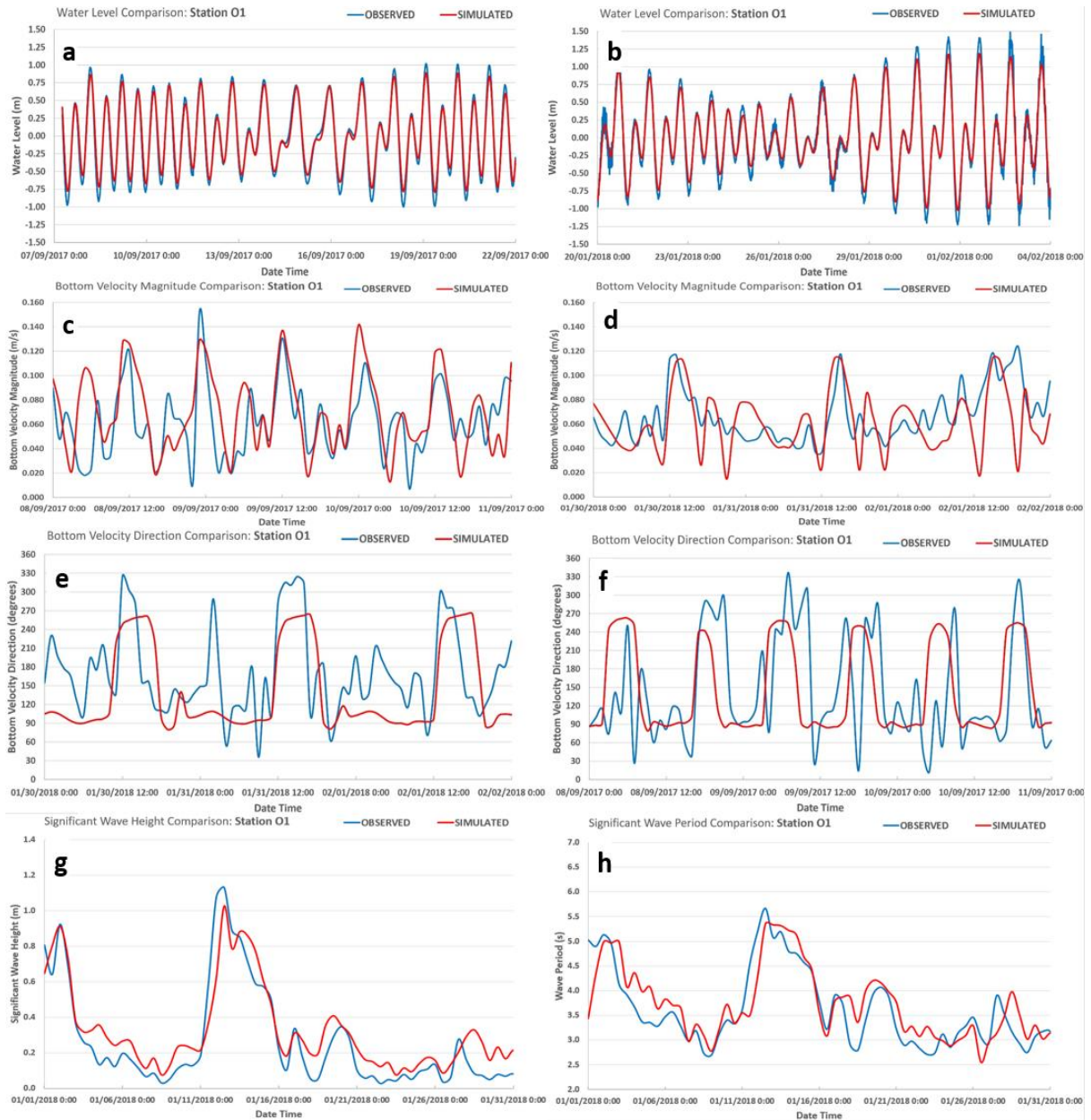
Figure 5. Comparison of simulated and observed parameters: (a, b) water levels, (c, d) bottom velocity magnitude, (e, f) bottom velocity direction, (g) significant wave height, and (h) significant wave period at O1 after calibration of the nearshore model
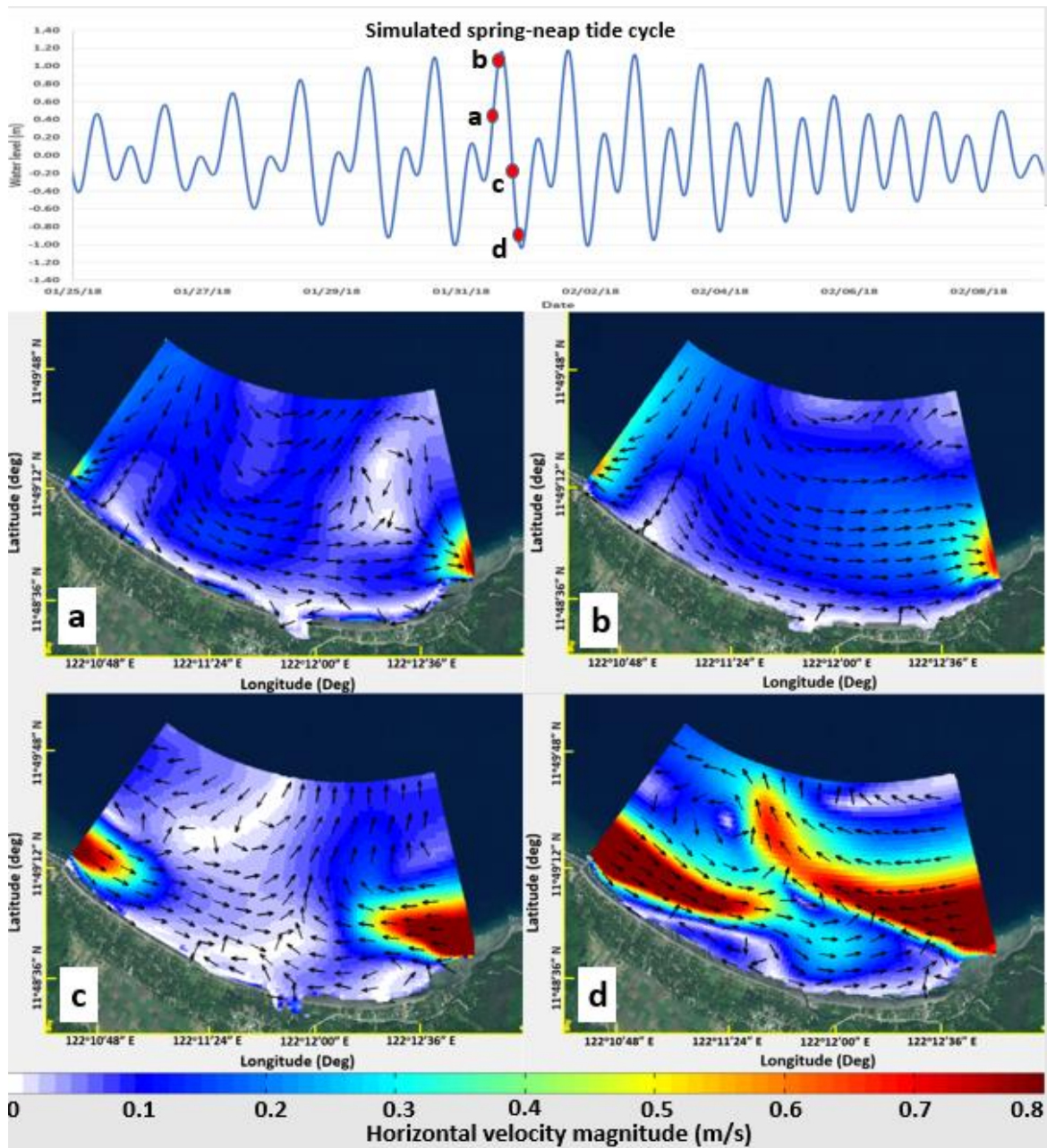
Figure 6. Simulated surface horizontal velocity patterns during: (a, b) flood and (c, d) ebb tide

The 3D simulation of the nearshore model offers an opportunity to examine further the near-bed velocity in the study area. The near-bed velocity, unlike depth-averaged and surface velocity, is more important to examine in morphological studies since it is the most accurate velocity to use in calculating bottom shear stress, the parameter which dictates the motion of the sediments in the bed. Figure 7 shows a snapshot of near-bed currents and surface currents at a same time step in the long-term simulation. In terms of direction, the near-bed currents follow the same path as those in the surface. In terms of the magnitude, however, the effect of the bed roughness significantly reduced the current speeds at the bottom by around 0.1 to 0.2

m/s. This difference is significant since the formulation of the bed shear stress magnitude is directly proportional to the square of the current speed.
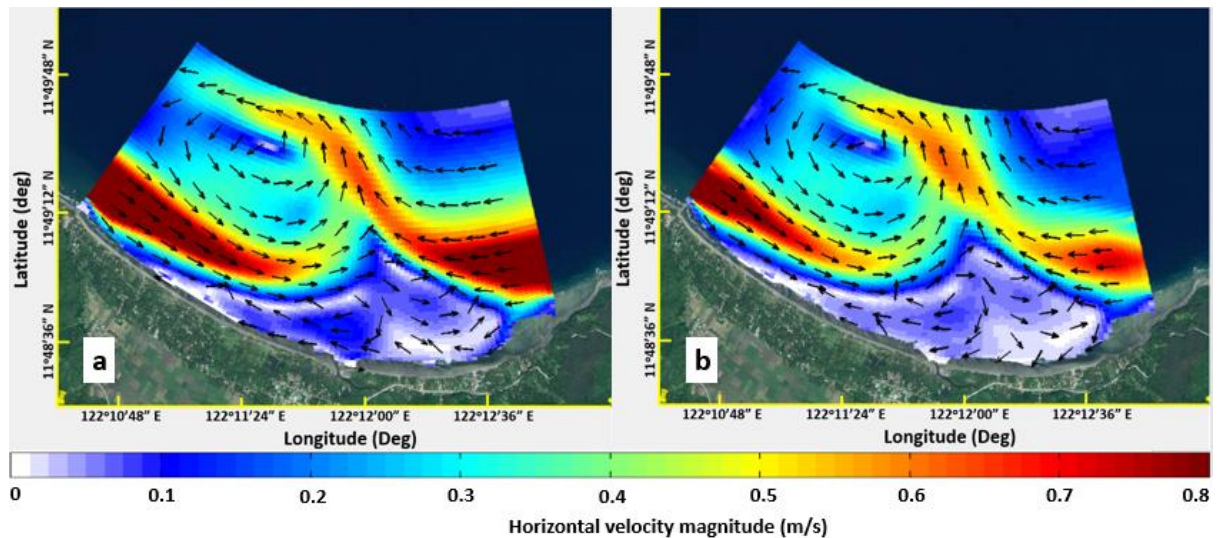
Figure 7. Comparison of the horizontal currents at the instant, February 2, 2018 00:00:00 UTC: (a) at the surface (top layer) and (b) near-bed (bottom layer)

3.2 Monsoonal Wind-generated Waves

   Waves propagating towards the study coast is greatly affected by seasonal monsoon winds. As shown in Figure 8, wave rose diagrams at O1 indicate a difference of at least 0.5 meters between the significant wave heights during the dry season when northeast monsoon winds are blowing (November to April) and the wave heights during the dry season when southwest monsoon winds (June to October) are present. All the waves are coming from the north to northeast direction where the Sibuyan Sea is situated.

   Wave breaking is an important process which drives the transport of sediments in the surf zone. Based on the plots shown in Figure 8, waves tend to break farther from the coast during the dry season months as the northeast monsoon winds amplify the energy carried by the waves, making it sufficient to break at deeper regions. The breaker line is more visible in the dry season months simulations compared to the wet season months.
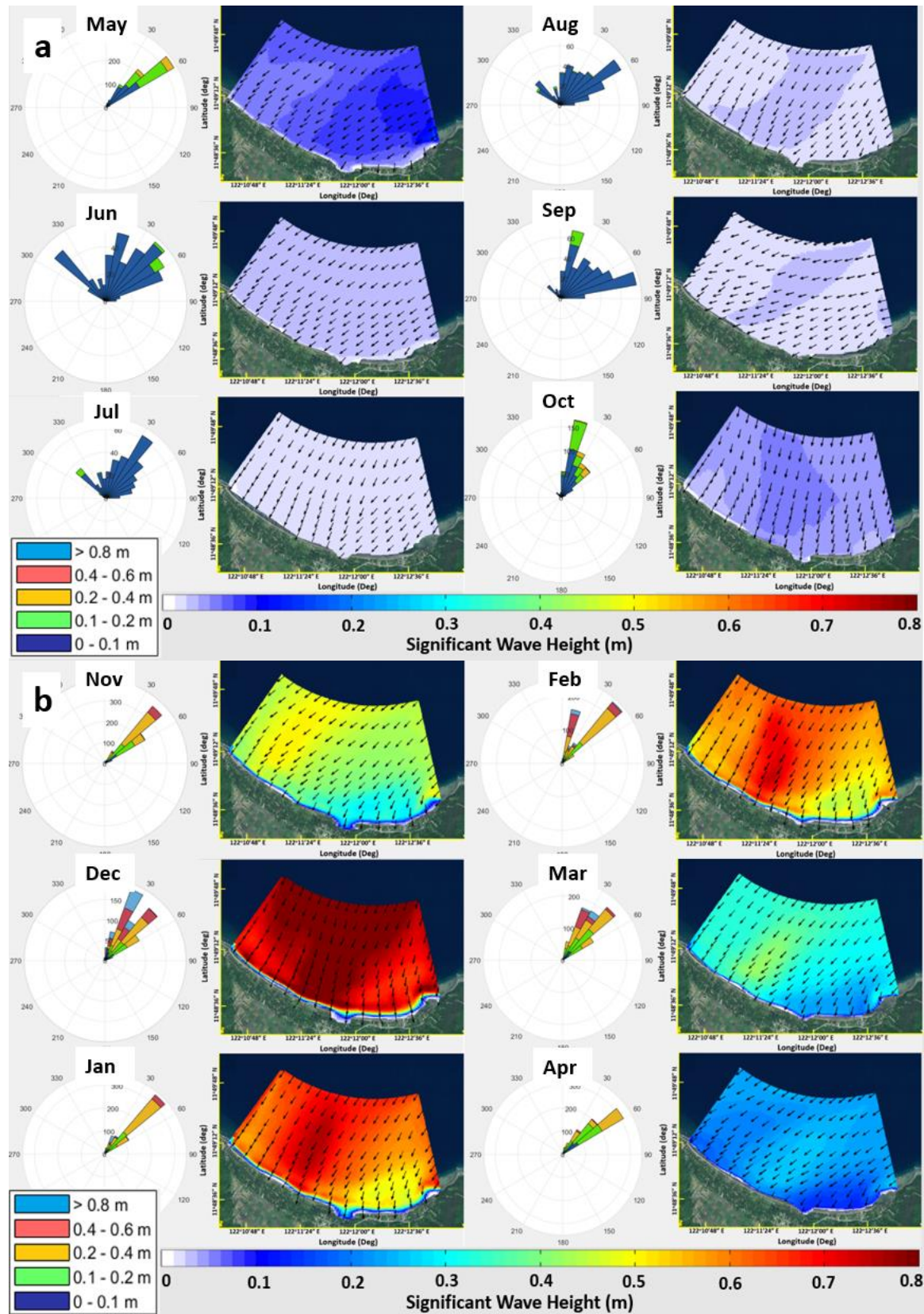
Figure 8. Significant wave height distribution and wave rose diagrams at O1: (a) during dry season months (May to Oct) and (b) during wet season months (Nov to Apr)

3.3 Effects on Morphological Dynamics

The long-term change in the morphology of the study area was analyzed by plotting the cumulative erosion and deposition for one year as shown in Figure 9. Areas of erosion and deposition were observed near the lateral boundaries and onshore.

The change in morphology observed in the lateral boundaries was caused by the tidal asymmetry between ebb and flood tide. During ebb flow, fast-moving currents travel towards the center of the domain from the lateral boundaries bringing along some sediments that were dragged from the shallow bed due to the induced bottom shear stress. When the tide transitions, relatively slower currents exit to the same lateral boundaries. Due to the difference in current speeds, the induced bottom shear stress could not take the same number of sediments back to its original position and these sediments settle at the area farther from the lateral boundaries where deposition is observed. The continuous tidal fluctuations caused erosion as much as 3 meters of sand in the area nearest to the lateral boundary and deposits 1-2 meters distributed along the direction of the currents. Unfortunately, the depth of erosion and deposition in the area cannot be verified with actual data. However, it is important to note that the amount of sediments that can be eroded is dependent on the thickness of the sediment layer which is a user-defined parameter that can be adjusted in the model.

Simulated morphological changes onshore are caused by the breaking of waves. Under a breaking wave, excessive turbulence produces a force that either slides or rolls the sediments along the bed (bedload transport) or uplifts the sediments and keep it into suspension through oscillatory motion of the regrowing wave. When the oscillatory motion cannot keep the sediment in suspension, it will settle on an area closer to the shore beyond the breaking line of the waves. The disturbed sediments will travel along the direction of the propagating wave which is why the observed erosion and deposition pattern is along the cross-shore direction.
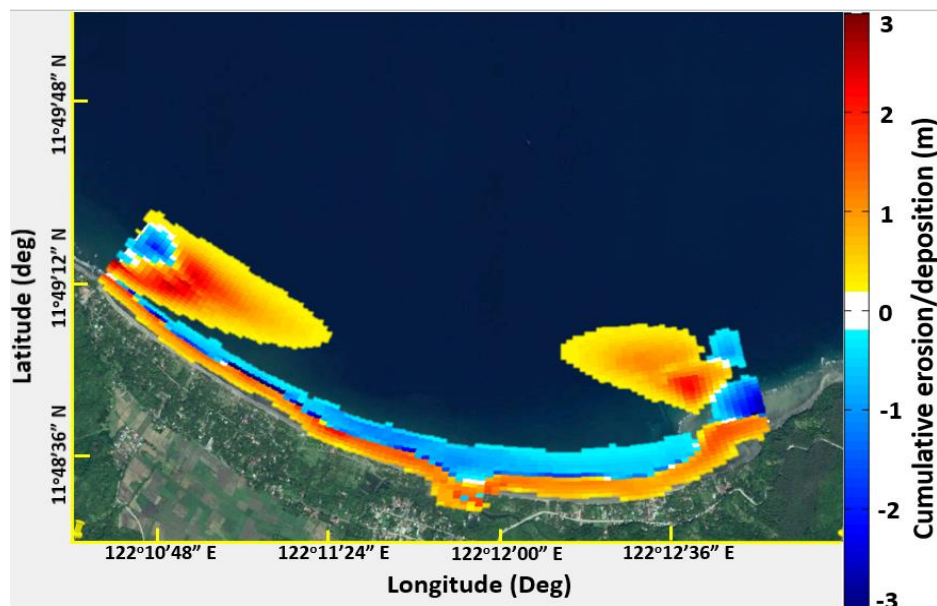
Figure 9. Cumulative erosion (blue patch) and deposition (red patch) in the study area after 1-year long simulation

The effects of the seasonal monsoon winds on the morphology changes are examined by running the nearshore model from November 1, 2017 to May 1, 2018 (dry season), the period when northeast monsoon winds are blowing. Figure 10 shows the cumulative erosion/deposition values obtained from this simulation and comparing with the year-long simulation on Figure 9, it can be observed that the sediment dynamics during the northeast monsoon season is more active, thus creating deeper erosions and thicker depositions in the same areas as the year-long simulations. Higher energy waves during the northeast monsoon season break in the surf zone causing more sediments to be eroded and deposited forward. This phenomenon of enhanced onshore-directed transport caused by breaking can be attributed to the skewness of the orbital velocity produced by the shoaling of waves [26]. The enhanced erosion and deposition at the lateral boundaries are attributed to the larger tidal range during dry season months. The highest tidal ranges occurred from November 2017 to February 2018 and during the months of April 2018 to July 2018. Majority of these months were included in the dry season simulation where the lowest ebb tide of around -1.1 meters is observed. The magnitude of the currents causing the transport of sediments at the lateral boundaries is higher as the tide level is lower which indicates that there are more instances of faster currents moving the sediments during the dry season (November to April) than that of the wet season (May to October). The difference in erosion and deposition between the dry season and 1-year long simulation is inferred to be the amount recovered during wet season.
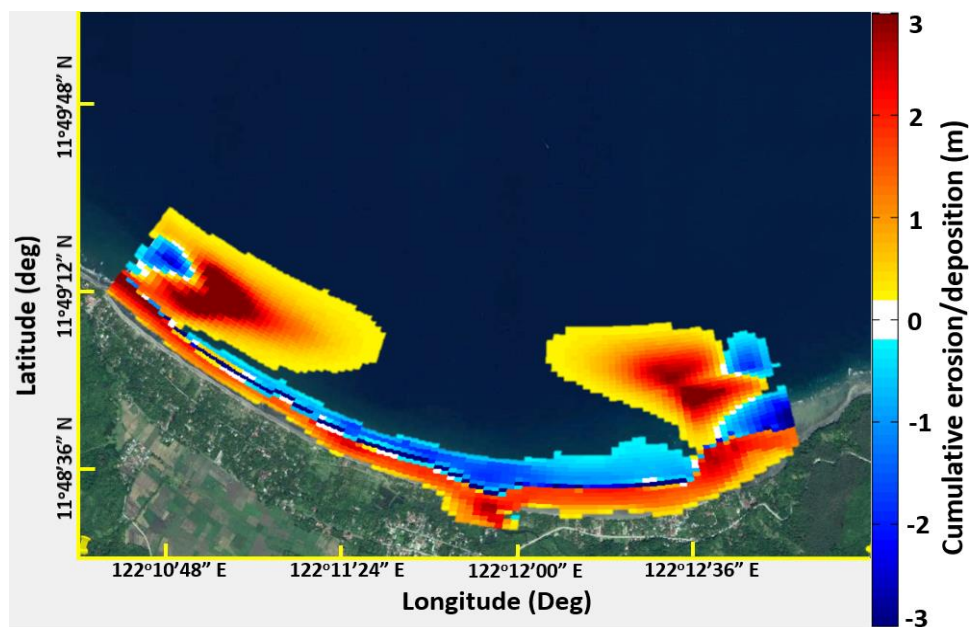
Figure 10. Cumulative erosion (blue patch) and deposition (red patch) in the study area from November 1, 2017, to May 1, 2018

Three beach profiles on different locations along the coast were extracted from the dry season and 1-year long simulation results and are shown in Figure 11. Section a-a is located on the right side, b-b is at the center, and c-c is on the left side of the study coastline. All three

profiles exhibited bed level changes along the cross-shore direction at the point where the breaking of waves is located while the profiles near the lateral boundaries (a and c) showed deposition a few hundred meters offshore. Eroded sediments under the breaking waves are being transported forward onshore and settles there forming a well-defined berm. After the dry season, the berm formed is larger but portions of it are recovered during the wet season by calm waves. The highest recovery during the dry season was observed in section a-a (or on the right side of the coast in general) due to the very mild slope causing the effects of the breaking of waves to be felt more by the bed than with a steeper slope like in sections b-b and c-c. Similarly, the areas at the outer nearshore close to the lateral boundaries are deposited with sediments during the dry season but are slightly eroded during the wet season.
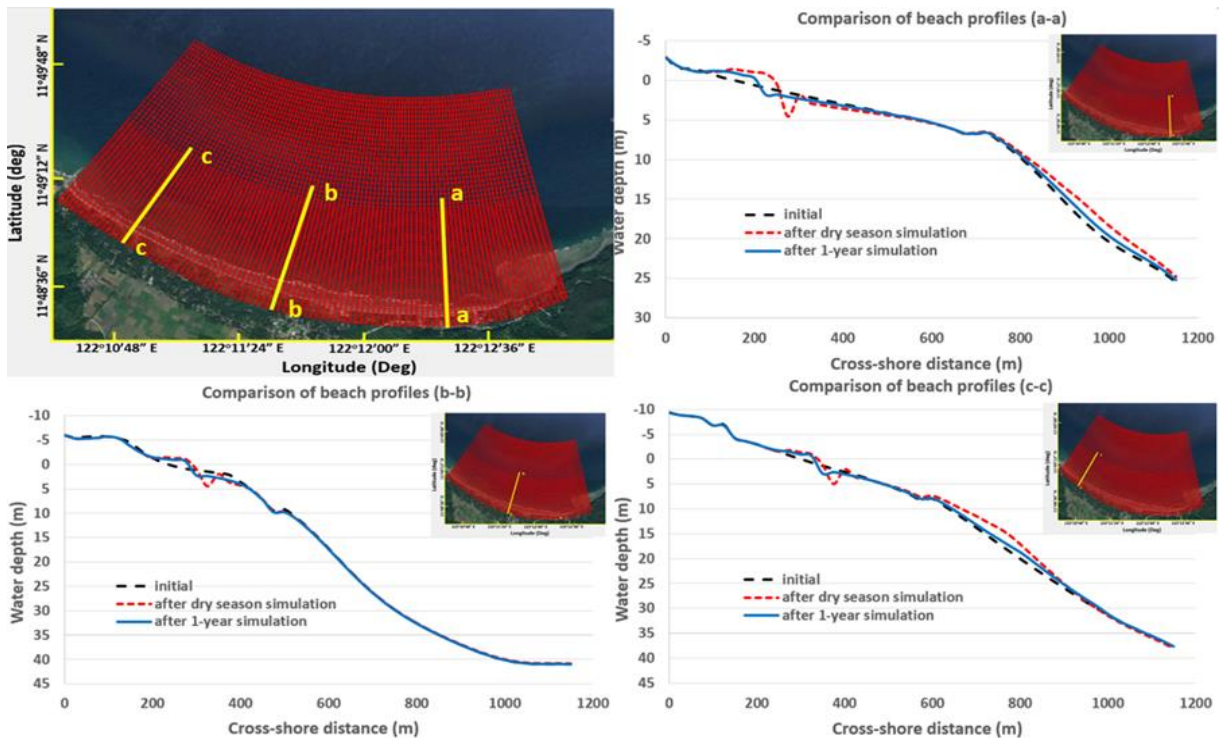
Figure 11. Cross-shore beach profiles at 3 different sections in the study coast after dry season and 1-year long simulations

The position of the shoreline (depth equal to zero) before and after the simulation can be traced from the nearshore model. The formation of the berm caused by the sand transport of waves adds more depth onshore causing the coastline to advance or move seaward. The presence of the wharf on the west and the headland on the east creates a controlled cell where sediments cannot escape. Longshore displacement of sand is also not observed which means that the coast is not eroding. In fact, the advance of the shoreline indicates that the coast is accreting. The rate of accretion cannot be determined however as calculating this actual quantity requires the calibration of the sediment transport model. Since coastal erosion is not present in the study area, engineering interventions such as construction of groins are not necessary anymore though it is possible to incorporate this scenario in the numerical model.

Figure 12. Position of the shoreline before and after the simulation

IV. CONCLUSIONS

A calibrated, coupled, hydrodynamic-wave model with sediment transport for the study area was successfully created using the Delft3D modelling suite. Three one-way nested computational domains were set-up using a combination of primary data from field surveys and secondary data obtained from various institutions. Prevailing coastal processes were characterized, and different patterns of velocity, waves, and sediment transport were described based on model simulation results. Furthermore, areas of erosion and accretion were identified based on the simulated cumulative erosion and deposition under prevailing conditions. Two sediment transport patterns were identified caused by tidal asymmetry and cross-shore wave action. Qualitative analysis of different beach profiles showed intensified movement of sediments during the dry season while for the rest of the months, recovery of sand was observed. Analysis of tracing of the shoreline indicated that the coast may be accreting under prevailing wind and wave conditions, despite the presence of coastal erosion indicators.

This study showcased the capability of numerical simulation as an important tool in assessing coastal morphodynamics and how it can be applied to deepen our understanding on the various physical processes happening in a coastal area. The methodology utilized in this research can be applied to other sites in the country provided that sufficient data are available to setup and calibrate the model. Water level, velocity, and wave properties are relevant data to simulate in characterizing coastal processes. In addition, calibration or validation of the sediment transport model expands the analysis to a quantitative approach in terms of sediment transport rates and bed level change predictions. Data such as time-varying suspended sediment concentration at different locations, seasonal monitoring of bathymetry, beach profile and shoreline position, long-term variation of bathymetry and topography published by NAMRIA, and suspended sediment concentration obtained from global satellite images, can be used for this endeavor. In the absence of primary data, secondary data from global data sets and local institutions can be used but with proper consideration to its effect on model

performance and reliability. Overall, this study incorporates all the necessary stages in developing a sophisticated Delft3D model and can be used as basis in analyzing the prevailing coastal processes on a specific local study area.

V. ACKNOWLEDGEMENTS

Nomenclature

DENR	Department of Environment and Natural Resources
DOST-ASTI	Department of Science and Technology – Advanced Science and Technology Institute
GEBCO	General Bathymetric Chart of the Oceans
GPS	Global Positioning System
NAMRIA	National Mapping and Resource Information Authority
RMSE	root-mean-square-error
SWAN	Simulating Waves Nearshore

References:

[1] Department of Environment and Natural Resources (DENR), Bureau of Fisheries and Aquatic Resources (BFAR) of the Department of Agriculture (DA) and Department of Interior and Local Government (DILG). 2001. Philippine coastal management guidebook no. 1: Coastal management orientation and overview. Coastal Resource Management Project of the Department of Environment and Natural Resources, Cebu City, Philippines, p. 58.

[2] Doroteo HJ. 2015. Disaster risk profile and disaster risk management framework of the Philippines: Natural disasters. Conference: Erasmus Mundus Master in Public Health in Disasters; University of Oviedo, Asturias, Spain. p. 1-46. 10.13140/RG.2.1.4656.3922

[3] Siringan FP, Sta. Maria MYY, Jordan JCJ. 2019. Coastal erosion management in the Philippines: A guidebook. The Marine Science Institute, University of the Philippines Diliman: Quezon City, Philippines. p. 155

[4] Sagip Baybay PH. 2018. Retrieved from https://sagipbaybayph.com/home/where-in-pinas/?fbclid=IwAR0MWkXe0QEbZClaLotYRmH3ErrEVbIvNcEHkjgRPrtBYdYaY8HVA3HmIm8 on 19 Oct 2018.

[5] Siringan FP, Berdin R, Sta. Maria Y. 2004. Coastal erosion in San Fernando, La Union: Trends, causes and possible mitigation measures [terminal report]. Marine Geology Laboratory, National Institute of Geological Sciences. University of the Philippines Diliman. p. 61.

[6] Perez R, Amadore L, Feir R. 1999. Climate change impacts and responses in the Philippines coastal sector. Climate Research. 12(2/3):97-107.

[7] Balce C, Leones J, De Leon P, Geosciences Bureau, Tacloban City, Philippines. 1999. Coastal erosion in

Eastern Leyte Island, Philippines [technical report]. Committee for Coordination of Joint Prospecting for Mineral Resources in Asian Offshore Areas (CCOP) 35th session Part II, UNDP Regional Offshore Prospecting in East Asia, Bangkok, Thailand. p. 84.

[8]   Bañas JC, Subade RF, Salaum DN, Posa CT. 2020. Valuing vanishing coasts: The case of Miagao coastline in Southern Iloilo, Philippines. Ocean & Coastal Management. 184(3):105008.

[9]   Economy and Environment Program for Southeast Asia (EEPSEA). Retrieved from http://www.eepsea.net/pub/rr/12511774031JKBayani_RR_2009-RR2.pdf on 19 July 2018.

[10]   Ringor CL, Siringan FP. 1998. Net sediment transport in Pampanga Bay, northwestern Manila Bay, derived from grain size trends, bathymetric change and landsat data. The Philippine Agricultural Scientist. 99(1):68-79.

[11]   Berdin R, Remotigue C, Zamora P. 2004. Coastal erosion vulnerability mapping along the southern coast of La Union, Philippines. Global Symposium for Hazard Risk Reduction: Lesson Learned from Applied Research Grants for Disaster Risk Reduction Program. 51-67.

[12]   Doruelo JS. 2000. The dynamics of sediment transport off the coast of Cavite [masteral]. University of the Philippines Diliman. p. 95.

[13]   Soria JA, Switzer AD, Pilarczyk JE, Siringan FP, Khan NS, Fritz HM. 2017. Typhoon Haiyan overwash sediments from Leyte Gulf coastlines show local spatial variations with hybrid storm and tsunami signatures. Sedimentary Geology. 358:121-138.

[14]   Doctor MA. 2018. Shoreline response of Eastern Leyte to single extreme event Super Typhoon Yolanda and to long-term forcing mechanisms [masteral]. University of the Philippines Diliman.

[15]   Mohamed Rashidi AH, Jamal MH, Hassan MZ, Mohd Sendek SS, Mohd Sopie SL, Abd Hamid MR. 2021. Coastal structures as beach erosion control and sea level rise adaptation in Malaysia: A review. Water. 13(13):1741.

[16]   Unguendoli S, Biolchi LG, Aguzzi M, Pillai UPA, Alessandri J, Valentini A. 2023. A modeling application of integrated nature-based solutions (NBS) for coastal and flooding mitigation in the Emilia-Romagna coastline (Northeast Italy). Science of the Total Environment. 867:161357.

[17]   Badru GS, Odunuga SS, Omojola AS, Oladipo EO. 2022. Numerical modelling of sediment transport in southwest coast of Nigeria: Implications for sustainable management of coastal erosion in the Bight of Benin. Journal of African Earth Sciences. 187:104466.

[18]   Lesser GR, Roelvink JA, van Kester JATM, Stelling GS. 2004. Development and validation of a three-dimensional morphological model. Coastal Engineering. 51(8-9):883-915.

[19]   Booij N, Ris R, Holthuijsen LH. 1999. A third-generation wave model for coastal regions. 1. Model description and validation. Journal of Geophysical Research. 104(C4):7649-7666.

[20]   Rijn LC van. 1993. Principles of sediment transport in rivers, estuaries and coastal seas. Aqua Publications. The Netherlands.

[21]   Rijn LC van. 2003. Sediment transport by currents and waves; general approximation formulae Coastal Sediments. In Corpus Christi. USA.

[22]   Komen GJ, Hasselmann S, Hasselmann K. 1984. On the existence of a fully developed wind-sea spectrum. Journal of Physical Oceanography. 14:1271-1285.

[23]   Zijlema M, van Vledder GP, Holthuijsen LH. 2012. Bottom friction and wind drag for wave models. Coastal Engineering. 65:19-26.

[24]   Williams JJ, Esteves LS. 2017. Guidance on setup, calibration, and validation of hydrodynamic, wave, and sediment models for shelf seas and estuaries. Advances in Civil Engineering. 5251902:25.

[25]   Chatzirodou A, Karunarathna H, Reeve DE. 2017. Modelling 3D hydrodynamics governing island-associated sandbanks in a proposed tidal stream energy site. Applied Ocean Research. 66:79-94.

[26]   Aagaard T, Hughes M, Ruessink, G. 2018. Field observations of turbulence, sand suspension, and cross-shore transport under spilling and plunging breakers. Journal of Geophysical Research: Earth Surface. 123(11):2844-2862.